Damage Detection in Composites by ZnO Sensors

H. J. Viljoen and N. F. J. van Rensburg
Dept. of Chemical Engineering, University of Nebraska-Lincoln, Lincoln, NE 68588

The development of composites with self-diagnostic capabilities is based on the analysis of a mathematical model of the structure. The method is illustrated for a vibrating cantilevered plate and analyzed considering damping. Damage is modeled as an elastic joint, and the spectrum of natural frequencies is calculated for different positions and magnitudes of the elastic joint. Small sensors consisting of tungsten filaments coated with ZnO are embedded in the plate, and their output is modeled. The solution of the inverse problem depends on the position and extent of damage which can be uniquely solved if the system is not overdamped with respect to the primary frequency. Higher modes have a decreasing contribution to the signal output; when the primary mode is overdamped, only the secondary frequency can be detected reliably. The solution to the inverse problem is no longer unique; there are as many as three different solutions (damage position and extent of damage) all of which produce the same signal output.

Introduction

The detection of cracks or damaged regions is one of the aspects in the development of smart materials attracting much interest. A further challenge is the estimation of the magnitude of the damage. Material structures which have the capability to do their own health-monitoring can be used as critical components in larger systems. Galea et al. (1993) conducted tests on carbon fiber/epoxy resin composites which form part of an aircraft. Polyvinylidene fluoride (PVDF) films were bonded to the surface of the composite. The specimens were externally loaded at a constant frequency. Fastener holes were then drilled and metal fixtures were fitted in them to simulate composite-to-metal joints. The amplitude of the output signal of the piezoelectric PVDF films were compared with the output for specimens without fastener holes. Damage detection was based only on changes in the amplitudes. Smaller films located near the damaged area showed bigger changes in amplitude ratio. This is expected, since the changes due to damage will be masked when sensors measure over a larger area.

PVDF films cannot be used for subcutaneous interrogation, and embedded sensors must be considered. However, there are two factors which weigh against embedded sensors. They can compromise the strength of the material and their mere presence can alter the strain field they are supposed to measure. The ideal embedded sensor must be unobtrusive and must have high strain to failure. Carman and Reifsnider (1993) suggested that the most plausible geometry to be used for embedded sensors is a continuous cylinder. The most popular choice for continuous cylindrical fibers is still optic fibers, although alternatives are being investigated, such as nitinol fibers. Another attractive alternative is ZnO-coated tungsten fibers. These coated fibers are outstanding in terms of their structural strength and small size. These sensors are almost unobtrusive towards the host material in terms of distorting the stress field, lowering the structural strength, or modifying microcrack distribution. A further advantage of the cylindrical sensor is its ability to measure the field locally. When sensors measure a field (thermally, chemically, or mechanically) over a relatively large area of the host material, local variations (or damage structure) can be masked by adjacent regions.

In this article we want to develop some ideas around the embedding of cylindrical sensors in a composite and the interpretation of signal output to detect the location and magnitude of damage. The basis of our approach is that locally damaged areas will cause a shift in the natural frequency spectrum. Adams et al. (1978) provides a good discussion on the advantages of natural frequency measurements over other nondestructive tests to detect damage in structures. When composites are damaged, an increase in damping and a reduction in stiffness are usually observed leading to changes in

N. F. J. van Rensburg is currently at the Dept. of Mathematics, University of Pretoria, Pretoria, South Africa.

the natural frequencies. This idea has been used by several researchers to detect damage in offshore structures (cf. references in Yuen, 1985). Other applications include the monitoring of rotating machines (Dimarogonas and Papadopoulos, 1983). Yuen (1985) analyzed a cantilevered beam by finite elements method. Damage was modeled as changes in the Young's modulus and both changes in frequencies and the shape of the eigenfunctions were calculated. Cawley and Adams (1979) also used finite elements to model the natural vibrations of a plate, and they developed a method of sensitivity analysis to find the location of the damage. Although good agreement was found with experimental results, the method requires considerable computing time and additional measurements to predict where the damaged area is located.

In previous studies on the shift in natural frequency spectra with increasing damage, two factors have not been addressed satisfactorily. The aspect of damage has either been modeled as a change in cross section (cf. Sato, 1983) or as changes in the Young's modulus (Yuen, 1985). We use the concept of an elastic joint to describe damage; it is mathematically well-defined and physical changes of the system can be easily related to our dimensionless parameter that quantifies the damage. The second aspect which has been largely overlooked, is the role of damping. It is known that damping affects the frequency (different types of damping affect the spectrum differently). To illustrate the methodology, a cantilevered plate is chosen. Viscous damping is also considered in the analysis. Damage (crack) is modeled as an elastic joint, and the spectrum of natural frequencies is calculated for different positions and magnitudes of the elastic joint. Small sensors consisting of tungsten filaments coated with ZnO are embedded in the plate and their output is modeled. The inverse problem is also addressed. We analyze the sensor output and try to identify the location of the elastic joint and its magnitude.

Model for Cantilevered Plate

We will only consider one-dimensional transversal vibrations. It is also assumed that the plate can be modeled as a one-dimensional continuum. Reismann (1988, p. 115) showed that in the case of pure bending, the solution for the plate problem approaches the solution for a beam as the width becomes smaller. In this study we will consider plates with aspect ratios L:W:H in the order of 10:1:0.1. Let λ_m denote the mass per unit length of the plate ($\lambda_m = \rho WH$) and the plate bending stiffness $D = E_x I$, where the moment of inertia $I = WH^3/12$. Defining the dimensionless variables $\xi = x/L$, $u = U/L$, and $\tau = t\sqrt{D/L^4\lambda_m}$, the transversal displacement is given by

$$\frac{\partial^2 u}{\partial \tau^2} = -\frac{\partial^4 u}{\partial \xi^4} - \alpha_D \frac{\partial u}{\partial \tau}. \tag{1}$$

The dimensionless viscous damping parameter α_D is defined in terms of the damping coefficient C as $CL^2/\sqrt{\lambda_m D}$. Damage in the plate will be modeled as an elastic joint. Consider a local section of the plate, with length $l \ll L$. In this section D differs from the rest of the plate and is denoted as D_l. Define

$$\delta = \lim_{l \to 0} \frac{lD}{D_l L} \tag{2}$$

as a dimensionless measure of the magnitude of the damage. The damage is modeled in a point, and it can be shown that the following jump condition holds across l

$$\left[\frac{\partial u}{\partial \xi}\right] = \delta \frac{\partial^2 u}{\partial \xi^2} \tag{3}$$

Note that $[\cdot] \equiv (\cdot)^+ - (\cdot)^-$. The problem can be solved using separation of variables, i.e, $u = X(\xi)T(\tau)$.

In dimensionless form, the damage is located at $\xi = \gamma$. The boundary conditions are

$$X = \frac{dX}{d\xi} = 0, \quad \xi = 0 \tag{4}$$

$$X = \left[\frac{dX}{d\xi}\right] - \delta \frac{d^2X}{d\xi^2} = \left[\frac{d^2X}{d\xi^2}\right] = \left[\frac{d^3X}{d\xi^3}\right] = 0, \quad \xi = \gamma \tag{5}$$

$$\frac{d^2X}{d\xi^2} = \frac{d^3X}{d\xi^3} = 0, \quad \xi = 1, \tag{6}$$

The eigenvalue problem

$$\frac{d^4X}{d\xi^4} = \lambda X \tag{7}$$

can be solved to find the eigenvalues λ_i. Although the values for λ_is are independent of α_D, they are influenced by δ and γ. The solution of $T(\tau)$ involves the following characteristic equation

$$\omega^2 + \alpha_D \omega + \lambda_i = 0. \tag{8}$$

If $\alpha_D^2 \geq 4\lambda_i$, the plate is overdamped and no oscillations of the ith mode will occur. It is clear that the primary eigenvalue is more likely to be damped than higher order modes.

We assume that the initial state is the equilibrium solution for a constant load at the free end

$$u(0, \xi) = h\left[\frac{3}{2}\xi^2 - \frac{1}{2}\xi^3\right], \quad \xi \leq \gamma \tag{9}$$

$$u(0, \xi) = h\left[\frac{3}{2}\xi^2 - \frac{1}{2}\xi^3 + 3\delta(1-\gamma)\xi - 3\delta(1-\gamma)\gamma\right], \quad \xi \geq \gamma \tag{10}$$

where h is a dimensionless displacement at the free end. The eigenfunctions are complete and can be used as a basis to approximate $u(0, \xi)$. For this choice of initial condition, the Fourier coefficients converge rapidly and the first four modes give a good approximation of the initial state.

The only parameter that is problematic to quantify is the damping coefficient C. Estimates can be obtained from ana-

lyzing experimental data, measuring the decay in amplitude. However, the parameter appears in the exponent and it is quite sensitive to inaccuracies. A further test to crosscheck C is to vary the free length of the plate and determine the length where the first mode becomes overdamped. Damping plays an important role in the inverse problem. For example, in overdamped systems, the parameters γ and δ cannot always be uniquely determined from sensor output.

Model for Sensor Output

When the plate vibrates freely, the stress tensor is given by

$$T = \begin{bmatrix} T_1 & 0 & T_5 \\ 0 & 0 & 0 \\ T_5 & 0 & 0 \end{bmatrix} \tag{11}$$

The strain tensor is given by

$$S = cT \tag{12}$$

where c is the compliance tensor for the composite material (Tsai, 1987). The sensor perturbs the stress field in its near vicinity, but we assume that this perturbation is negligible, due to the small dimensions of the sensor. We further assume that no slip occurs across the composite and ZnO interface (perfect bonding). Therefore, strain is continuous. The strain tensor has to be transformed to a cylindrical coordinate system concurrent with the sensor (r^c, θ, y^c). The transformation matrix is given by

$$A = \begin{bmatrix} \cos\theta\cos\alpha & \cos\theta\sin\alpha & 0 \\ -\sin\alpha & \cos\alpha & 0 \\ \sin\theta\cos\alpha & \sin\theta\sin\alpha & \cos\theta \end{bmatrix}. \tag{13}$$

In Figure 1 the system is shown with the sensor positioned at a distance z_p from the neutral plane and at an angle α with respect to the positive y-axis. We will distinguish variables in the cylindrical coordinate system by a superscript c. Hence the transformed strain tensor is given by

$$S^c = ASA^T. \tag{14}$$

where A^T is the transposed matrix.

It is also assumed that no electric fields exist in the azimuthal and axial directions of the ZnO film and the c-axis of the polycrystalline film is oriented in the radial direction. (This assumption is quite valid in light of the strong self-texturing of ZnO to grow normal to the c-axis on both amorphous and single crystal substrates.) Under open-circuit conditions, the following relationship holds for the radial component of the dielectric displacement vector

$$\int D_r^c dA = 0. \tag{15}$$

where $\int dA$ is evaluated over the surface of the sensor. It follows from the relation between dielectric displacement, electric field and strain

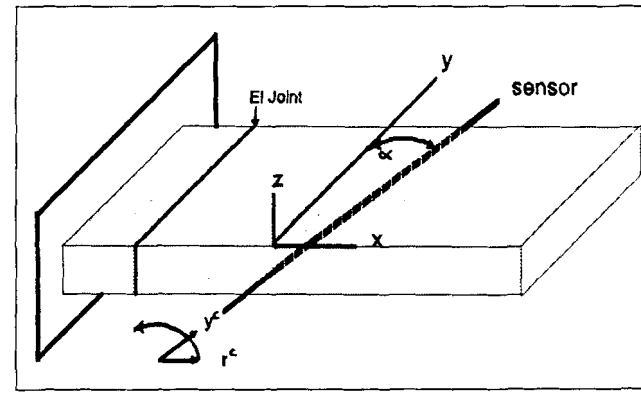

Figure 1. Cantilevered plate.

$$D_r^c = \epsilon_{zz}^S E_r^c + e_{z1} S_{\theta\theta}^c + e_{z3} S_{rr}^c + e_{z1} S_{zz}^c \tag{16}$$

that the electric field between the tungsten and the carbon fiber is given by

$$E_r^c = -\frac{\int \left[\frac{e_{z1}}{\epsilon_{zz}^S} S_{\theta\theta}^c + \frac{e_{z1}}{\epsilon_{zz}^S} S_{zz}^c + \frac{e_{z3}}{\epsilon_{zz}^S} S_{rr}^c \right] dA}{\int dA}, \tag{17}$$

The permittivity and piezoelectric stress tensors are given by ϵ and e respectively (Auld, 1982). If the film thickness is h_f, the signal output can be estimated in volt: $V = E_r^c h_f$. In evaluating the integrals of Eq. 17, we neglect angular variations in strain. Strictly speaking, the stresses are smaller at the point where the sensor surface is closer to the neutral plane and larger where the sensor is farther away from that plane. If the sensor diameter is small in comparison to the distance z_p angular variations can be neglected.

Results

A plate constructed from carbon fiber and epoxy resin is modeled. The plies are placed longitudinally in the X-direction of the composite. The free end is displaced by a dimensionless distance of 5% (real distance = $0.05 \times L$). The first four eigenfunctions are used to approximate the initial condition. The elastic joint can be easily conceptualized as a line along the width of the plate, where some fibers have been damaged or the epoxy resin has cracked.

The working example is a plate measuring 100 mm × 15 mm × 1.5 mm. Suppose a sensor of length $\mathcal{L} > L$ is placed with its center $(\mathcal{L}/2)$ at the point $(\xi, y) = (L/2, W/2)$. As the sensor is pivoted around its center from $\alpha = 0$ to $\alpha = 90°$, the length of the sensor that is embedded varies from W to L. In Figure 2 the maximum output is shown for sensors positioned at values of α between 0° and 90°. It must be noted that the coupling will differ for other types of loading (other than bending). If more sophisticated models are used, which would be appropriate for plates with different dimensions (two-dimensional models), the coupling effect will be different. The strongest coupling is found when the sensor is placed

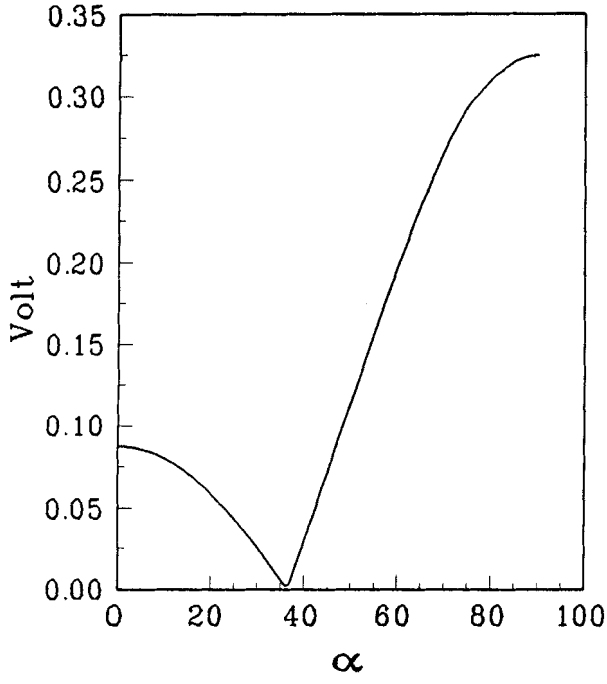

Figure 2. Effect of sensor position on signal output.

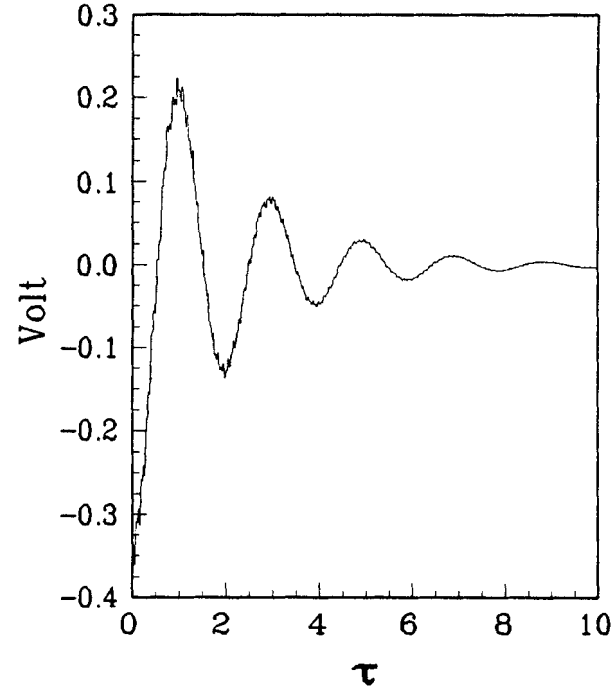

Figure 3. Sensor P1 signal.
$\gamma = 0.25$, $\delta = 0.1$.

longitudinally along the plate; very little coupling is observed for placement angles between 35°–40°.

Sensor output and damage

Define P1, P2 and P3 as the following three sensor positions:

P1: Sensor placed at $(\gamma - 0.01, 0°)$

P2: Sensor placed at (0, 90°).

Note that the position vector consists of the axial position and the angle w.r.t. the Y-axis. In Figures 3 and 4 the sensor output is shown for P1 and P2 respectively. In this case $\gamma = 0.25$, and the damage level δ is 0.1. The dimensionless damping coefficient is taken as $\alpha_D = 1$. The output of a third sensor (P3) placed at (0.75, 0°) is shown in Figure 5. Sensors P1 and P2 measure the primary frequency well, but higher modes are not really significant; however, it is sensor P3 that measures most of the higher mode interaction.

It is clear that transverse sensors positioned near the fixed end measure predominantly the primary frequency; higher frequencies are better detected when the sensor is positioned near the free end. This observation becomes especially important for systems where the primary frequency is overdamped. In overdamped systems, the only useful information will be obtained from sensors placed near the free end, albeit a much weaker signal. There are two reasons why longitudinal sensors extending along the full length of the plate measure primarily the first frequency. The contribution of the first mode dominates the total output (cf. Fourier coefficients for initial displacement) and strain is a maximum near the fixed end.

In Figure 6 the output is shown for an undamaged beam. The sensor is placed at (0.75, 0°), and the same damping coefficient was used as in the previous cases. A comparison of Figures 5 and 6 gives a good indication of the differences between an undamaged and damaged beam. Although small quantitative differences exist between the signals of damaged and undamaged plates, it is far from obvious to draw any physically meaningful conclusions from such a comparison.

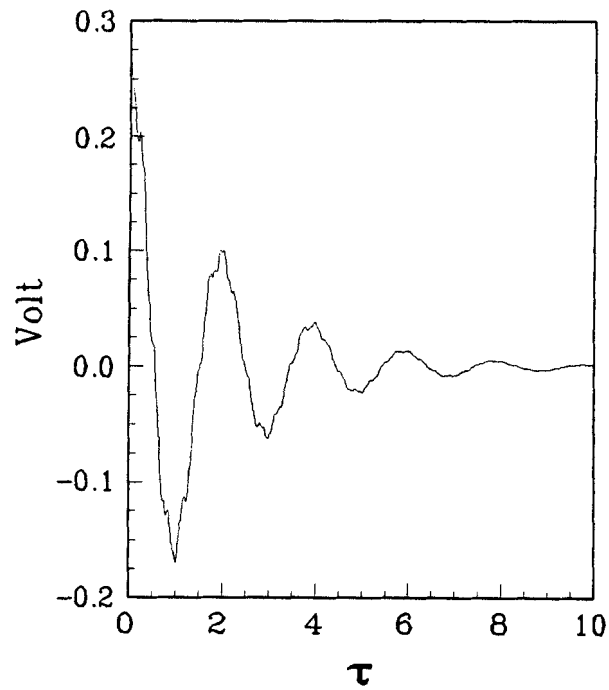

Figure 4. Sensor P2 signal.
$\gamma = 0.25$, $\delta = 0.1$.

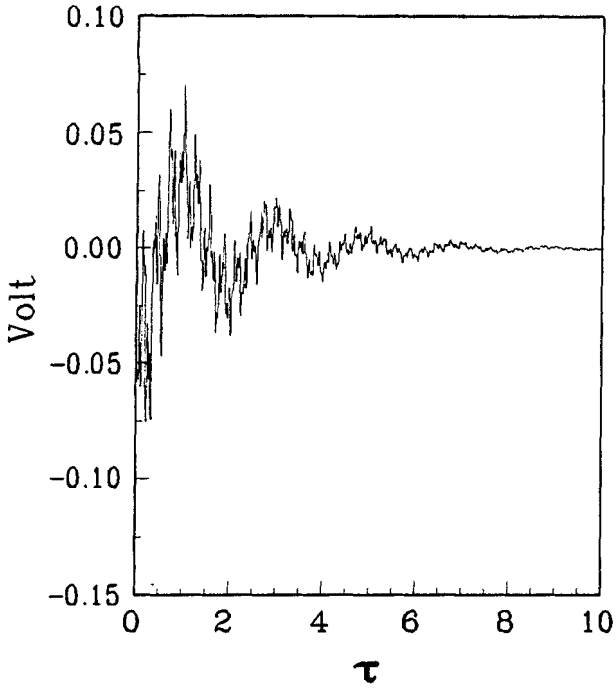

Figure 5. Sensor P3 signal.

$\gamma = 0.75$, $\delta = 0.1$.

More distinct changes exist between the natural frequency spectra of damaged and undamaged plates. In Figures 7 and 8 the primary and secondary frequencies are shown as functions of δ and γ. The functions show a sensitivity towards damage position and magnitude of damage. These observations lay the basis for the inverse problem.

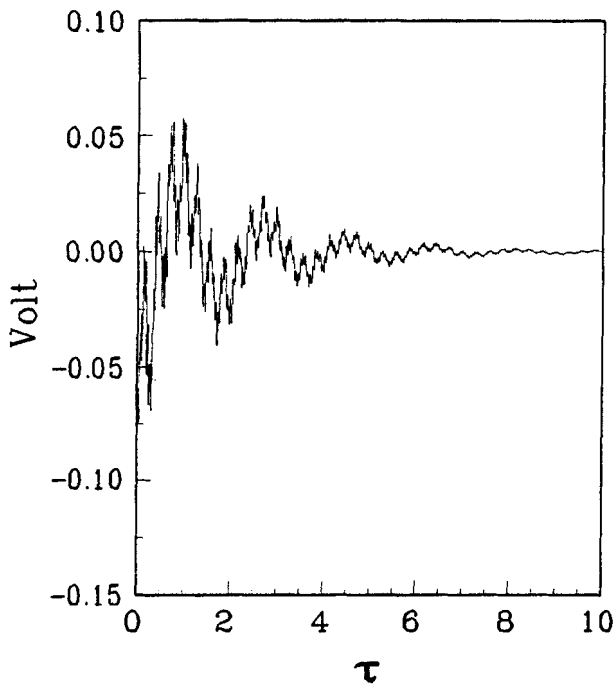

Figure 6. Undamaged plate.

Sensor at (0.75, 0°).

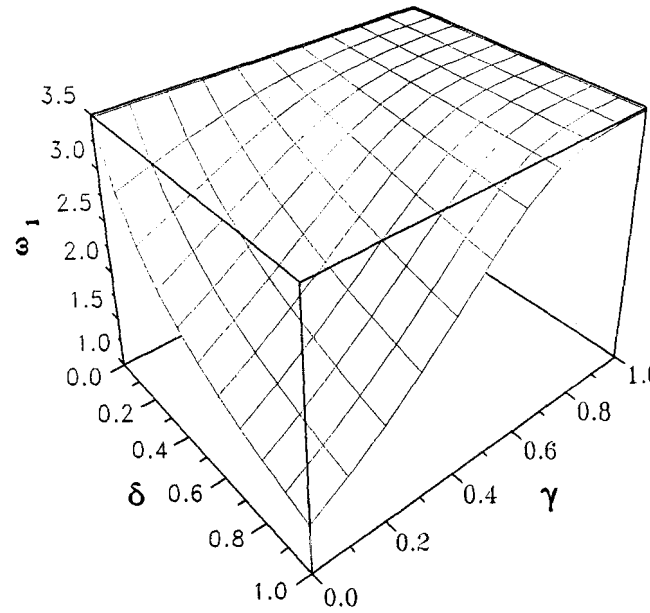

Figure 7. Primary frequency vs. γ and δ ($\alpha_D = 1$).

Inverse problem

The solution to the inverse problem will provide us with the position of the damage and the level of damage, but first we must investigate the uniqueness of the inverse mapping. The damage is exactly described by the location of damage (γ) and the extent of the damage (δ). It follows that we need two relations. The first one is obtained from a static test. Consider the change in static deflection at the free end for the same load as a damaged beam

$$u_{\text{damaged}} - u_{\text{intact}} = 3\delta h(1-\gamma)^2 \tag{18}$$

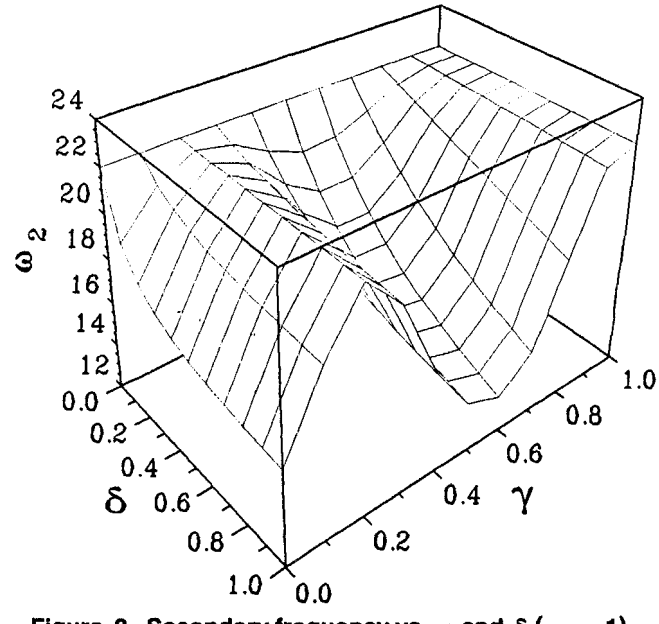

Figure 8. Secondary frequency vs. γ and δ ($\alpha_D = 1$).

A static test will provide a relationship between the extent of the damage (δ) and the position of the damage (γ). A second relation is necessary to define δ and γ uniquely, and it is obtained from solving the eigenvalue problem. We can substitute δ in terms of γ from Eq. 18 and calculate $\omega(\gamma, \delta(\gamma))$ from Eqs. 7 and 8.

Example. To illustrate the solution of the inverse problem, consider the following (hypothetical) case:

A system similar to our working example has a damping coefficient of $\alpha_D = 1$. A static test of the system, based on a 5% deflection of the free end, gives the following result (see Eq. 18)

$$u_{\text{damaged}} - u_{\text{intact}} = 0.0131$$

The Fourier transforms of the output of two sensors placed at (0.75, 0°) and (0.25, 0°) respectively, give $(\omega_1, \omega_2) = (3.08, 21.2)$. The frequencies differ from the values for an intact beam, and we want to determine the location and magnitude of the damage.

It follows from Eq. 18, that we can write δ in terms of γ. The eigenvalue problem can then be solved for the primary frequency over a range of γ-values. The result is shown in Figure 9. Note that the function is monotone, and the position of the damage can be read from the graph at $\omega = 3.08$. Both sensors indicate the damage to be positioned at $\gamma = 0.12$. From Eq. 18, it then follows that $\delta = 0.13$.

Now, suppose the primary frequency is not known. A very likely reason is that the system is overdamped with respect to the primary mode of vibration. The eigenvalue problem is solved for the secondary frequency $\omega_2 = \omega_2[\gamma, \delta(\gamma)]$, and the result is shown in Figure 10. The sensor measured a secondary frequency (dimensionless) of 21.1. If one correlates this frequency with γ, it follows from Figure 10 that there are three different possible solutions.

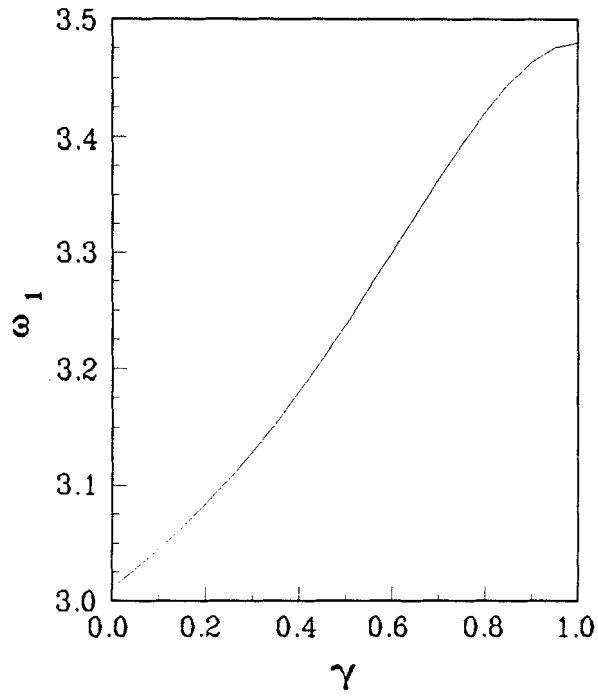

Figure 9. Projected primary frequency.

Conclusions

A model for a cantilevered plate has been used as an example to develop some ideas for the manufacture of a materials system with self-diagnostic capabilities. All the ideas are based on the assumption that a mathematical model exists which accurately describes the behavior of the system. We have modeled the signal output of ZnO-coated cylindrical sensors placed at arbitrary positions in the plate. Sensor output is sensitive towards the position of the sensor in the system. Damage is introduced in the form of an elastic joint, and in this study we limit the analysis to one dimension. Therefore, damage can be uniquely described by the position of the elastic joint and the magnitude of the jump condition at the joint provided the damping coefficient is known.

Comparing damaged and intact systems small quantitative changes are observed in the signal output, but it is found that noticeable frequency shifts occur. The shift in natural frequencies offers an attractive way to detect damage.

Sensors placed near the free end of the plate better measure higher-order frequencies, and this fact becomes especially important in overdamped systems when the inverse problem is addressed. Using information of a static test, the damage level can be expressed in terms of the position of the elastic joint (γ). The eigenvalue problem can be solved for different values of γ and for different frequency modes. Correlating primary frequencies with the eigenvalues, the inverse problem can be uniquely solved. However, if no data on primary frequencies are available, or if the system is overdamped with respect to the primary frequency, then the solution to the inverse problem is no longer unique.

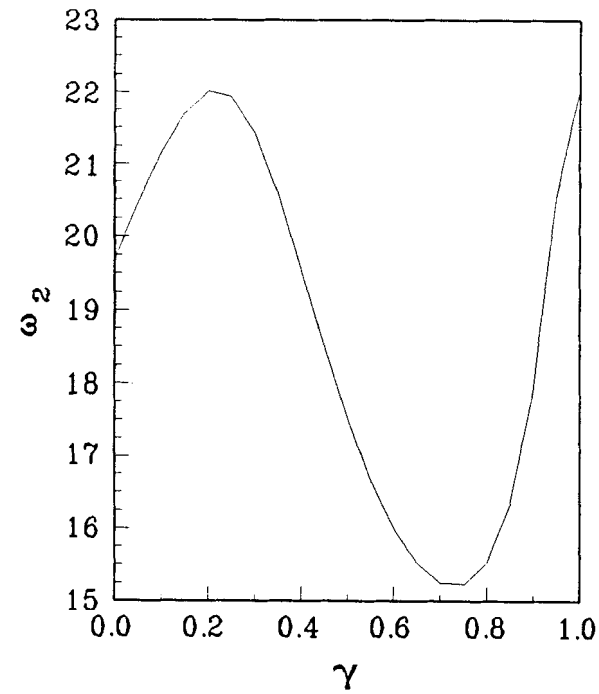

Figure 10. Projected secondary frequency.

Notation

A = transformation matrix defined by Eq. 13
c = compliance tensor, 1/Pa
C = damping coefficient, kg/m·s
D = plate flexural rigidity $E_x I$, Pa·m^4
D_r^c = radial component of dielectric displacement vector, C/m^2
e_{zi} = elements of z-component of piezoelectric stress tensor, C/m^2
E_r^c = radial component of electric field, V/m
E_x = longitudinal Young's modulus
h_f = thickness of ZnO film, m
H = thickness of plate
l = length of damaged section, m
L = length of plate, m
S = strain tensor
T = stress tensor, Pa
u = dimensionless transversal displacement, U/L
U = transversal displacement, m
x = axial distance, m
X = eigenfunction defined in Eq. 7
y = dimensionless transversal distance
t = time, s
W = width of plate, m
z_p = distance between neutral plane of plate and sensor, m

Greek letters

α = angle between sensor and *Y-axis* of plate
γ = dimensionless position of damage
δ = dimensionless measure of damage, defined in Eq. 2
ϵ_{zz}^c = normal z-component of permittivity tensor, F/m
θ = angular variable in cylindrical coordinate system
λ_m = mass per unit length of plate, kg/m
λ = eigenvalues of Eq. 7
ξ = dimensionless axial distance, x/L
ρ = density of plate, kg/m^3
τ = dimensionless time, $t/\sqrt{D/L^4\lambda_m}$
ω = dimensionless frequency, defined by Eq. 8

Literature Cited

Adams, R. D., P. Cawley, C. J. Pye, and B. J. Stone, "A Vibration Technique for Non-destructively Assessing the Integrity of Structures," *J. Mech. Eng. Sci.*, **20**, 93 (1978).

Auld, B. A., *Acoustic Fields and Waves in Solids*, Wiley, New York (1982).

Carman, G., and K. Reifsnider, "Analytical Optimization of Coating Properties for Actuators and Sensors," *J. Intelligent Mat. Syst. and Struc.*, **4**, 89 (1993).

Cawley, P., and R. D. Adams, "The Location of Defects in Structures from Measurements of Natural Frequencies," *J. Strain Analysis*, **14**, 49 (1979).

Dimarogonas, A. D., and C. A. Papadopoulos, "Vibration of Cracked Shaft in Bending," *J. Sound and Vibration*, **91**, 583 (1983).

Adams, W. D., P. Cawley, C. J. Pye, and B. J. Stone, "Use of Piezoelectric Films in Detecting and Monitoring Damage in Composites," *J. Intelligent Mat. Syst. and Structures*, **4**, 330 (1993).

Reismann, H., *Elastic Plates: Theory and Application*, Wiley, New York (1988).

Sato, H., "Free Vibrations of Beams with Abrupt Changes of Cross Sections," *J. Sound and Vibration*, **89**, 59 (1983).

Tsai, S. W., *Composites Design*, Think Composites, Dayton, OH (1987).

Yuen, M. M. F., "A Numerical Study of the Eigenparameters of a Damaged Cantilever," *J. Sound and Vibration*, **103**, 301 (1985).

Manuscript received Feb. 16, 1995, and revision received July 24, 1995.